Polymer Chemistry

ROYAL SOCIETY OF CHEMISTRY

COMMUNICATION

View Article Online
View Journal | View Issue

Check for updates

Cite this: *Polym. Chem.*, 2021, **12**, 2987

Received 4th January 2021,
Accepted 30th March 2021

DOI: 10.1039/d1py00013f

rsc.li/polymers

An unexpected role of an extra phenolic hydroxyl on the chemical reactivity and bioactivity of catechol or gallol modified hyaluronic acid hydrogels†

Sumanta Samanta,[a] Vignesh K. Rangasami,[a] N. Arul Murugan,[b] Vijay Singh Parihar,[a] Oommen P. Varghese[c] and Oommen P. Oommen*[a]

We present here a new insight into the chemical reactivity and bioactivity of dopamine (DA) and gallic acid (GA) and their hyaluronic acid (HA) conjugates. Our data suggest that HA–GA scaffolds are superior to HA–DA, with higher oxidation kinetics, improved tissue adhesive properties, and radical scavenging ability with a lower pro-inflammatory response.

Dopamine (DA) and Gallic acid (GA) hold a key position in material science, biology, and medicine as they possess diverse functional properties needed for applied sciences and technologies.[1–4] Although these polyphenols differ mainly in one phenolic –OH, they possess different properties. DA is an important neurotransmitter synthesized in the brain and kidney and regulates several cellular processes such as insulin production, vasodilation, lymphocyte activation, *etc.*[5,6] On the other hand, GA is found in fruits and medicinal plants, providing antioxidant properties.[7,8] Both these molecules also possess several common characteristics such as radical scavenging capabilities[9] and are used as anti-inflammatory agents, antimicrobial agents, antineoplastic agents, and neuroprotective agents.[7,10] DA and polyDA have been extensively studied in material science as they form mussel-inspired adhesives on wet surfaces.[11,12] However, very few studies are reported with GA.[13]

Under aqueous conditions, the reaction between DA and free radicals can follow two possible reaction mechanisms, namely; direct attack of radicals on DA leading to forming a DA-radical adduct (also known as hydrogen atom transfer or HAT mechanism) or follow proton abstraction from phenolic –OH groups followed by radical reaction (also known as sequential proton-loss electron transfer or SPLET mechanism).[14] To understand which pathway is favorable for the radical formation in DA and GA, we performed computational studies (B3LYP/6-311+G** level of theory and by using CPCM model for describing aqueous solvent medium) to estimate the energetics associated with HAT mechanism and SPLET mechanism (Fig. 1). We used *N*-protected DA and carboxy-functionalized GA for our computational study in order to minimize the interference from the carboxylate and amine functional groups.

To compute the free energy change associated with deprotonation reaction at neutral pH in water in both DA and GA derivatives, we used the equilibrium reactions as shown in eqn (1). Using this equilibrium, the pK_a's were computed from the free energy differences using eqn (2).[15] The details about calculations of energies for different molecular structures for DA

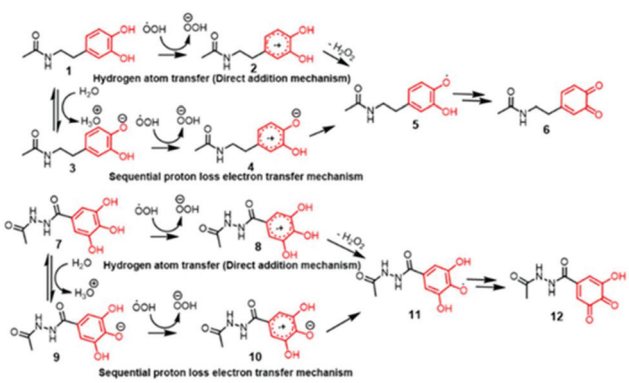

Fig. 1 Schematic representation of oxidation reaction of dopamine and gallic acid.

[a]*Bioengineering and Nanomedicine Lab, Faculty of Medicine and Health Technology, Tampere University, 33720 Tampere, Finland. E-mail: oommen.oommen@tuni.fi*
[b]*Department of Theoretical Chemistry and Biology, School of Engineering Sciences in Chemistry, Biotechnology and Health, KTH Royal Institute of Technology, S-106 91 Stockholm, Sweden*
[c]*Translational Chemical Biology Laboratory, Polymer Chemistry Division, Department of Chemistry, Ångström Laboratory, Uppsala University, 75121 Uppsala, Sweden*

†Electronic supplementary information (ESI) available. See DOI: 10.1039/d1py00013f

and GA namely, neutral, anion, dianion forms, free radical, and diradical forms are given in Tables S1–S3 in ESI.†

$$\text{Ar–OH} + \text{H}_2\text{O} \rightleftharpoons \text{H}_3\text{O}^+ + \text{Ar–O}^- \quad (1)$$

$$\text{p}K_\text{a} = \Delta G^*_\text{aq}/2.303\,\text{RT} \quad (2)$$

Consistent with the reported literature,[16] these calculations after zero-point error corrections indicated the pK_a of phenolic proton of DA at the *meta* position as 9.1 while that for the *para* position was 10.3 with the corresponding Gibbs free energy changes of 52.53 and 59.25 kcal mol^{-1} respectively. Intriguingly, the pK_a of the corresponding GA derivatives were found to be 8.31 (*para* position) and 8.66 (*meta* position) which corresponds to Gibbs free energy changes of 47.46 and 49.79 kcal mol^{-1} respectively. Notably, the phenolic –OH at the *meta* position has a lower pK_a in DA, whereas the phenolic –OH at the *para*-position has a lower pK_a in GA. The lower pK_a of GA is presumably due to the unique stabilization of the phenolate anion through intramolecular hydrogen bonding *via* two *meta* –OH groups in GA, resulting in a smaller hydrogen bond dissociation enthalpy.[17]

Next, we computed the energetics for the generation of radicals from neutral DA molecule (1 → 2 transitions) following the HAT mechanism and compared it with the energy required for 3 → 4 transformations following the SPLET mechanism (Fig. 1). Interestingly, the generation of free radicals from anion (3 → 4 transitions) was found to be more favorable than the single electron transfer from the neutral DA (1 → 2 transitions), as the free energy change observed was −297.38 kcal mol^{-1} when compared to −9.09 kcal mol^{-1} for the latter case. A similar trend was seen for GA derivatives where 9 → 10 transition, was an easier pathway than the radical reaction with a neutral GA molecule (7 → 8 transitions). The free energy changes for the two transitions were −291.3 and −7.78 kcal mol^{-1} respectively. This suggests the SPLET mechanism is thermodynamically favored over the one-electron transfer (HAT) mechanism. Thus, the pK_a of phenolic –OH in DA and GA would be the key factor that governs the chemical reactivity and bioactivity of these molecules (Fig. 2).

To validate our hypothesis, we synthesized the hyaluronan conjugates of DA (HA–DA) and GA (HA–GA) and estimated the pK_a of these conjugates by spectrophotometric methods.[18] Hyaluronic acid (HA) has been extensively studied to formulate nanocarriers[19–21] and hydrogels[11,12,22] for various drug delivery and tissue regenerative applications. We conjugated DA to the carboxylate groups on HA by carbodiimide coupling following our reported procedure.[12] To conjugate GA, we first modified GA carboxylate to hydrazide derivative before conjugating with HA by carbodiimide chemistry. The reactivity of hydrazide is higher than that of amines in the carbodiimide coupling due to the lower pK_a of hydrazides over amines enabling the reaction in acidic pH. However, the stability of the two products after conjugation is high. The degree of modification for DA and GA was tuned to be 4–5% with respect to the disaccharide repeat units. The spectroscopic analysis of the HA derivatives indicated a sigmoidal curve of the absorbance *vs.* pH for both HA–DA and HA–GA solutions (Fig. S12†). The graphical representation of $-\log[(A_{max} - A_i/A_i)]$ *versus* pH in Fig. 3A displays the pK_a values of the modified HA derivatives where the linear fit crosses the abscissa.

Fascinatingly, the pK_a estimated using the spectroscopic methods revealed a pK_a of 7.42 and 6.9-units in the case of HA–DA and HA–GA respectively which is roughly 1.4 and 1.7 units less than the computationally estimated values. This could be attributed to the H-bonding between the carboxylates in HA and phenolic –OH groups, assisting in faster deprotonation of the acidic phenolic proton, as observed previously with HA–thiol derivatives.[18] The observed pK_a values suggest that ~76% of HA–GA exist in the anionic state whereas only ~48% of HA–DA anionic mole fraction would exist under equilibrium at physiological pH (7.4), following Henderson–Hasselbalch equation (see section 1.5 in ESI†).

To understand the impact of the pK_a difference, we next elucidated the relative antioxidant properties of native GA and DA and as well as HA–GA and HA–DA conjugates using 2,2-diphe-

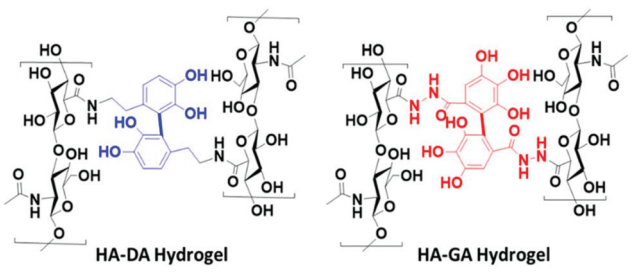

Fig. 2 Schematic representation of oxidation mediated hydrogel formation.

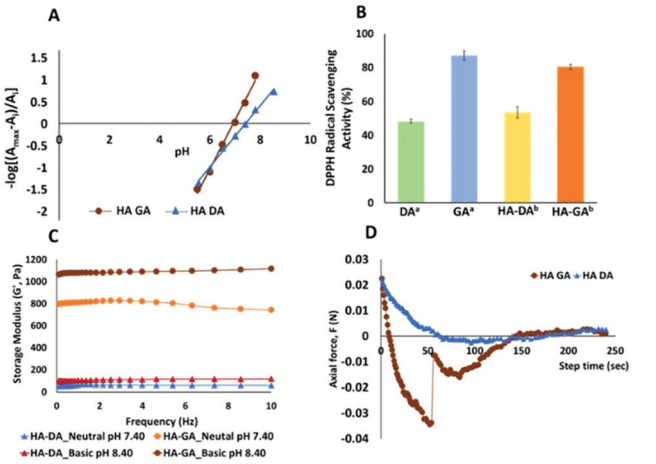

Fig. 3 (A) Logarithmic representation of the normalized absorbance ($-\log[(A_{max} - A_i)/A_i]$) as a function of the pH for HA–GA and HA–DA. (B) DPPH radical scavenging activity of DA and GA conjugated HA, free DA, and free GA. (*a* = 12.5 μM and *b* = 25 μM) (C) Comparative storage modulus of HA–DA and HA–GA hydro-gel under neutral and basic pH at a periodate mole ratio of 0.5 : 1 (D) tack adhesion force comparison of the hydrogels to porcine muscle.

nyl-1-picrylhydrazyl (DPPH) radical scavenging assay.[23] As anticipated, GA and HA–GA exhibited ~30% and ~27% higher radical scavenging capabilities than DA and HA–DA at 12.5 μM and 25 μM concentrations respectively (Fig. 3B). Since ~76% of HA–GA exists in the anionic state at physiological pH, we anticipated that the dissolved oxygen in the buffer could contribute to accelerating radical generation following eqn (3).

$$4\text{Ar–O}^- + \text{O}_2 + 4\text{H}_3\text{O}^+ \rightarrow 4\text{Ar–O}^- + 6\text{H}_2\text{O} \quad (3)$$

To ascertain this hypothesis, we first dissolved HA–DA and HA–GA (1.6 weight%) in phosphate buffer at pH 7.4 and pH 8.4 and determined hydrogel formation. Notably, at pH 7.4 and 8.4, the HA–GA solution demonstrated hydrogel formation in the absence of an initiator or oxidants with a storage modulus ~42 and ~100 Pa respectively (Table 1). HA–DA on the other hand did not show any hydrogel formation. However, when we dispersed HA–GA in a deoxygenated buffer at pH 8.4 and pH 7.4, we did not observe any gelation even after 2 h, signifying the role of molecular oxygen in promoting radical formation. We then evaluated the hydrogel formation with the HA derivatives in the presence of sodium periodate ($NaIO_4$) at physiological pH (pH 7.4) and basic conditions (pH 8.4). The HA–DA conjugate did not form any gels at neutral or basic pH when 0.1 moles of $NaIO_4$ were used relative to DA in HA ($NaIO_4$: DA in HA = 0.1 : 1). Interestingly, under the same conditions, the HA–GA derivative gave excellent gels with a storage modulus of 238 Pa and 346 Pa at neutral and basic pH respectively. When we increased the $NaIO_4$ concentration to 0.5 moles relative to DA ($NaIO_4$: DA in HA = 0.5 : 1) in the HA–DA solution, we obtained weak gels of 60–100 Pa at neutral and basic conditions. As anticipated, HA–GA gels on the other hand displayed over a 10-fold increase in mechanical strength of 800–1000 Pa range, under identical conditions.

We further evaluated the effect of crosslinking on enzymatic stability by performing a degradation study in presence of 25 U ml^{-1} hyaluronidases (section 1.10 and Fig. S14 in ESI†). For this study, we utilized HA–DA and HA–GA gels of nearly identical modulus (~340 Pa; *i.e.*, 0.1 : 1 $NaIO_4$: GA @ pH 8.4 and 1.5 : 1 $NaIO_4$: DA @ pH 8.4) and compared it with an HA–GA gel with the higher modulus (~800 Pa; 0.5 : 1 $NaIO_4$: GA @ pH 7.4). Interestingly, HA–GA gels displayed higher enzymatic stability than HA–DA gels.

Since DA-functionalized hydrogels are well-known as tissue adhesive materials, we next elucidated the relative tissue adhesive properties of HA–DA and HA–GA hydrogels following the rheometric tack-adhesion test. Compared to HA–DA, the HA–GA gels displayed significantly higher tack adhesion as it required more tensile force to separate the contacts between porcine tissue glued on the top geometry and hydrogel surface placed on the bottom plate resulting in more negative axial force (Fig. 3D, and Videos 1, 2 in ESI†). This implies that HA–GA gels possess stronger secondary interactions resulting in improved binding to the tissue when compared to the HA–DA gels. We also evaluated the biocompatibility of the two matrices by culturing human fibroblast cells (CRL-2429) within the hydrogels and performed the live/dead staining. Both HA–DA and HA–GA gels exhibited high cell viability without eliciting any significant toxicity at different time points (Fig. 4A, B, and Fig. S15 in ESI†), suggesting that both gels are biocompatible.

Finally, we investigated the effect of DA, GA, HA–DA, and HA–GA conjugates on human blood monocyte cells THP-1, to study if these molecules promote the differentiation of monocytes to macrophages, the key immune cells that dictate inflammation, implant integration, or rejection. Monocyte cells are non-adherent and upon differentiation to macrophages they become adherent. To our surprise, the incubation of our test agents with THP-1 cells triggered the differentiation of these cells to macrophages as they become adherent after treatment. We systemically investigated if the differentiated macrophages were of pro-inflammatory M1 or anti-inflammatory M2 phenotype by quantifying the mRNA expression of key cytokines namely, TNF, IL-1β, IL-1Ra, by qRT-PCR (Fig. 4C–F). Since HA itself is bioactive and induces macrophage polarization,[20,24] we compared HA–DA and HA–GA relative to unmodified HA.

Interestingly, all the test agents displayed elevated levels of pro-inflammatory markers (M1 markers)[25] such as IL-1β, however, this effect was prominent for DA and HA–DA than for GA-based materials. On the other hand, the GA and HA–GA displayed lower TNF and elevated levels of anti-inflammatory IL-1Ra expression relative to DA and HA–DA. This implies DA and DA-derived materials possess pro-inflammatory characteristics (M1 phenotype) while the GA and GA-derived materials possess predominately anti-inflammatory M2 phenotype with

Table 1 The storage modulus of HA–DA and HA–GA hydrogels

	HA–DA gels		HA–GA gels	
$NaIO_4$: DA/GA (mole ratio)	Neutral pH (7.4)	Basic pH (8.4)	Neutral pH (7.4)	Basic pH (8.4)
No $NaIO_4$	X[a]	X[a]	G' = 42 ± 17 Pa	G' = 100 ± 27 Pa
No $NaIO_4$ (deoxygenated)[b]	X[a]	X[a]	X[a]	X[a]
0.1 : 1	X[a]	X[a]	G' = 238 ± 20 Pa	G' = 346 ± 16 Pa
0.5 : 1	G' = 346 ± 16 Pa	G' = 104 ± 7 Pa	G' = 810 ± 20 Pa	G' = 1080 ± 12 Pa
1 : 1	G' = 211 ± 12 Pa	G' = 290 ± 7 Pa	X[c]	X[c]
1.5 : 1	G' = 262 ± 11 Pa	G' = 325 ± 6 Pa	X[c]	X[c]

[a] No gel formed. [b] Components dissolved in the degassed buffer. [c] Extremely fast gelling kinetics.

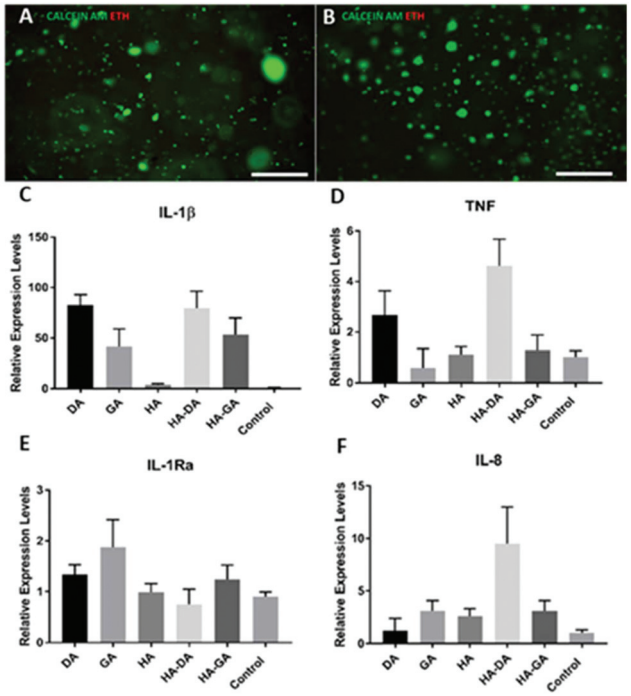

Fig. 4 Live/dead staining of CRL-2429 cells in (A) HA–DA (pH 8.4) and (B) HA–GA (pH 7.4) hydrogel after 7 days in culture; mRNA expression levels of (C) IL-1β, (D) TNF, (E) IL-1Ra and (F) IL-8 genes by THP-1 cells after 8 days in culture with the different hydrogel components.

some pro-inflammatory characteristics. GA has high antioxidation property, therefore helps in inhibiting reactive oxygen species (ROS) production, which in turn reduces inflammatory cytokine productions. We also measured the levels of IL-8, a potent chemoattractant for neutrophils,[26] and a key stimulator of angiogenesis. Surprisingly, HA–DA displayed elevated levels of IL-8 suggesting implantation of HA–DA-based materials would promote neutrophil infiltration and trigger angiogenesis.

In conclusion, we found that an extra phenolic –OH at the active site of GA reduces the pK_a of GA, which results in an accelerated rate of oxidation (by SPLET mechanism), radical reaction, and antioxidant property. Unlike HA–DA, the HA–GA conjugate facilitated fast hydrogel formation by air oxidation and required a 15-fold lower $NaIO_4$ concentration than HA–DA to obtain hydrogel with comparable viscoelastic properties. The HA–GA hydrogel system also displayed a significantly higher tissue adhesive property than HA–DA-derived hydrogel. Both DA, GA, and their HA conjugates differentiated monocytes to macrophages, although DA treated macrophages displayed higher expression of proinflammatory cytokines while the GA derivative displayed a more anti-inflammatory phenotype. To the best of our knowledge, this is the first report on the direct comparison of DA and GA and their HA-derivatives. We believe our results provide new insight into the mechanism and activity of DA and GA derivatives, which implies that GA-based materials possess a clear advantage over DA-based materials for biomedical applications.

Author contributions

OPO has conceptualized, supervised, and wrote the original draft with the help of all authors. SS, VKR, and NAM are responsible for data curation, formal analysis, investigation, and writing the manuscript. OPV reviewed and edited the original draft as necessary.

Conflicts of interest

The authors declare no conflicts of interest.

Acknowledgements

We acknowledge Dr Vijay Singh Parihar for assisting in the synthesis of the hydrazide derivative of gallic acid. We also acknowledge Begona Morras for assisting with the rheological measurement of the gels. SS thanks to the European Union's Horizon 2020 Marie Sklodowska-Curie Grant Program (Agreement No. 713645) for the financial support.

References

1 M. Shin and H. Lee, *Chem. Mater.*, 2017, **29**, 8211–8220.
2 J. Y. Lai and L. J. Luo, *Biomacromolecules*, 2015, **16**, 2950–2963.
3 J. Yang, M. A. Cohen Stuart and M. Kamperman, *Chem. Soc. Rev.*, 2014, **43**, 8271–8298.
4 P. Das and N. R. Jana, *RSC Adv.*, 2015, **5**, 33586–33594.
5 H. Juárez Olguín, D. Calderón Guzmán, E. Hernández García and G. Barragán Mejía, *Oxid. Med. Cell. Longevity*, 2016, 2016.
6 T. Hussain and M. F. Lokhandwala, *Exp. Biol. Med.*, 2003, **228**, 134–142.
7 B. Badhani, N. Sharma and R. Kakkar, *Review Gallic acid: A versatile antioxidant with promising therapeutic and industrial applications, RSC Adv.*, 2015, **5**, 27540–27557.
8 A. Chanwitheesuk, A. Teerawutgulrag, J. D. Kilburn and N. Rakariyatham, *Food Chem.*, 2007, **100**, 1044–1048.
9 T. Marino, A. Galano and N. Russo, *J. Phys. Chem. B*, 2014, **118**, 10380–10389.
10 M. Kaur, B. Velmurugan, S. Rajamanickam, R. Agarwal and C. Agarwal, *Pharm. Res.*, 2009, **26**, 2133–2140.
11 J. Shin, J. S. Lee, C. Lee, H. J. Park, K. Yang, Y. Jin, J. H. Ryu, K. S. Hong, S. H. Moon, H. M. Chung, H. S. Yang, S. H. Um, J. W. Oh, D. I. Kim, H. Lee and S. W. Cho, *Adv. Funct. Mater.*, 2015, **25**, 3814–3824.
12 L. Koivusalo, M. Kauppila, S. Samanta, V. S. Parihar, T. Ilmarinen, S. Miettinen, O. P. Oommen and H. Skottman, *Biomaterials*, 2019, **225**, 119516.
13 K. Zhan, C. Kim, K. Sung, H. Ejima and N. Yoshie, *Biomacromolecules*, 2017, **18**, 2959–2966.
14 H. W. Richter and W. H. Waddell, *J. Am. Chem. Soc.*, 1983, **105**, 5434–5440.

15 T. Marino, A. Galano and N. Russo, *J. Phys. Chem. B*, 2014, **118**, 10380–10389.
16 R. Romero, P. R. Salgado, C. Soto, D. Contreras and V. Melin, *Front. Chem.*, 2018, **6**, 1–11.
17 J. S. Wright, E. R. Johnson and G. A. DiLabio, *J. Am. Chem. Soc.*, 2001, **123**, 1173–1183.
18 D. Bermejo-Velasco, A. A. Azémar, O. P. Oommen, J. Ns Hilborn and O. P. Varghese, *Biomacromolecules*, 2019, **20**(3), 1412–1420.
19 O. P. Oommen, J. Garousi, M. Sloff and O. P. Varghese, *Macromol. Biosci.*, 2014, **14**, 327–333.
20 V. K. Rangasami, S. Samanta, V. S. Parihar, K. Asawa, K. Zhu, O. P. Varghese, Y. Teramura, B. Nilsson, J. Hilborn, R. A. Harris and O. P. Oommen, *Carbohydr. Polym.*, 2020, 117291.
21 J. M. Jones, D. J. Player, S. Samanta, V. K. Rangasami, J. Hilborn, M. P. Lewis, O. P. Oommen and V. Mudera, *Biomater. Sci.*, 2020, **8**, 302–312.
22 A. Sigen, Q. Xu, P. McMichael, Y. Gao, X. Li, X. Wang, U. Greiser, D. Zhou and W. Wang, *Chem. Commun.*, 2018, **54**, 1081–1084.
23 J. Y. Lai and L. J. Luo, *Biomacromolecules*, 2015, **16**, 2950–2963.
24 J. E. Rayahin, J. S. Buhrman, Y. Zhang, T. J. Koh and R. A. Gemeinhart, *ACS Biomater. Sci. Eng.*, 2015, **1**, 481–493.
25 L. Dugo, M. G. Belluomo, C. Fanali, M. Russo, F. Cacciola, M. MacCarrone and A. M. Sardanelli, *Oxid. Med. Cell. Longevity*, 2017, **11**, 6293740.
26 G. A. Duque and A. Descoteaux, *Front. Immunol.*, 2014, 5.